Multidiszciplináris tudományok, 13. kötet. 3. sz. (2023), pp. 257-267 **https://doi.org/10.35925/j.multi.2023.3.25**

DETERMINING THE QUALITY FACTOR OF SANDSTONE USING ACOUSTIC LABORATORY MEASUREMENTS

Brigitta Turai-Vurom
PhD student, University of Miskolc, Institute of Exploration Geosciences, Department of Geophysics
3515 Miskolc-Egyetemváros, e-mail: brigitta.vurom@gmail.com

Mihály Dobróka
professor emeritus, University of Miskolc, Institute of Exploration Geosciences, Department of Geophysics
3515 Miskolc-Egyetemváros, e-mail: dobroka@uni-miskolc.hu

Abstract

The paper presents the velocity-pressure and quality factor-pressure dependences of a sandstone sample, using the Fourier spectra of the complete waveforms of the P waves measured in laboratory. Measurements were performed on sandstone and (a reference) aluminum sample at 40 different pressures. The professional literature uses approximate methods to determine the value of the quality factor. The spectral ratio method was used to evaluate our measurements. The measured velocity and quality factor data were processed using inversion methods. The results showed that both the velocity-pressure and the quality factor pressure dependence can be well-described utilizing the double relaxation model in forward modeling.

Keywords: *acoustic P wave measurements, quality factor, velocity and quality factor inversion, double relaxation*

1. Introduction

The methods based on the propagation of elastic waves can be used in several fields, during laboratory tests, but also in the field of raw material explorations, during borehole acoustic geophysical profiling, and even in the field of archaeology. The examination of acoustic waves generated under laboratory conditions has many advantages, since the measurements can be carried under controlled pressure- and temperature conditions. This is important because changes in pressure affect acoustic propagation velocities and the attenuation of elastic waves. In the knowledge of the pressure dependence we can estimate the pressure (pore pressures) under real condition (Dócs and Baracza, 2022; Nagy et al., 2019; Nagy et al., 2021). Additional important parameters can be derived from these petrophysical parameters and the dynamic elastic moduli can also be specified. As the pressure increases, the pore space in the rock begins to close (Birch, 1960), the microcracks close (Walsh and Brace, 1964), and the longitudinal (P) and transversal (S) wave propagation velocities increase as a result of the rock compaction. It is well known that in acoustic wave propagation has a strong pressure dependence (Wyllie et al., 1958; Nur and Simmons, 1969; Stacey, 1976). Many empirical forms have been created to describe this physical phenomenon, but we cannot fully accept them as models providing a real physical explanation. At increasing pressure, in the range of low pressures, the acoustic velocity increases rapidly, then the rate of increase gradually decreases, reaching a maximum value at high pressures (Birch, 1960; Yu et al., 1993). This phenomenon occurs due to changes in the rock structure, compression of pores (Birch, 1960;

Jones and Wang, 1981) and closure of cracks (Walsh and Brace, 1964; Sengun et al., 2011). In the acoustic laboratory test, the propagation velocities (Vp and Vs) of pressure waves (P waves) and shear waves (S waves) are measured as a function of pressure (P) on core samples. The Department of Geophysics of the University of Miskolc has been conducting significant research and development in this field for several decades. New petrophysical model was introduced (Dobróka and Somogyi Molnár, 2012). The new model has been used to describe both the pressure dependence of P waves (Somogyi Molnár et al., 2015) and that of S waves (Kiss, 2018). The new models were further developed for two-component (Somogyi Molnár et al., 2019) and multi-component (Dobróka et al., 2022) relaxation cases. Another frequently studied and important phenomenon is the attenuation of waves (absorption coefficient – $\boldsymbol{\alpha}$) and the quality factor ($\boldsymbol{Q}$) defined by the relationship of Knopoff (1965) as follows:

$$\alpha = \frac{\pi f}{v_f Q} \tag{1}$$

where f – the frequency in *Hz*,
v_f – the velocity measured in *m/s*.

The theories describing the pressure dependence of the velocities can also be used to describe the relationship between the quality factor and pressure, since as a result of the increasing pressure, when the microcracks close, the individual grains get closer to each other, so the value of the measurable absorption coefficient decreases, and the value of the quality factor increases similarly to the model of the acoustic velocity. The time-domain signals of the acoustic waves (the full wave images) can be transformed into the frequency domain, and the characteristics of the spectra produced in this way can be examined. The spectrum and spectral ratio of the core samples (Diallo et al., 2003) can be calculated as a function of frequency in relation to the spectrum of the aluminum reference sample. Using the fact that aluminum has a very high quality factor, the quality factor of rocks can be calculated from the spectral ratios (Knopoff, 1965; Toksöz et al., 1979). In this paper, we determined the pressure dependence of the quality factor of the sandstone sample using the improved method of Toksöz. The velocity-pressure and quality factor-pressure dependences were inverted using the single and double relaxation models.

2. Acoustic velocity measurements

In the Rock Physics Laboratory of the Geophysics Department of the University of Miskolc, we performed additional, more detailed measurements (with a higher pressure range and resolution) compared to the measurements presented the previous year (Turai-Vurom and Dobróka, 2022). We recorded the complete P- and S-wave images on the sandstone sample and measured them in the pressure range of *0.26–82.153 MPa* at *40* discrete pressures (*0.26, 1.04, 3.12, 5.2, 7.279, 9.359, 11.439, 13.519, 15.599, 17.678, 19.758, 21.838, 23.918, 25.998, 28.077, 30.157, 32.237, 34.317, 36.397, 38.477, 40.556, 42.636, 44.716, 46.796, 48.876, 50.955, 53.035, 55.115, 57.195, 59.275, 61.354, 63.434, 65.514, 67.594, 69.674, 71.754, 73.833, 75.913, 80.073 and 82.153 MPa)*. The full waveform was also measured on the reference aluminum sample at all 40 discrete pressures. We determined the quality factor (*Q*) of the sandstone sample by calculating spectral ratios from the spectra obtained after Discrete Fourier Transformation (DFT) of the measured waveforms.

3. Determining the quality factor using the method of spectral ratios

In addition to the propagation velocity of acoustic waves, the attenuation of the waves (absorption coefficient) and the quality factor associated with it are often investigated and important phenomena. There are several models to describe the attenuation in the international literature, the Biot model (Biot, 1956), (Birch, 1960), the viscoelastic model (Bland, 1960), and the elastic dispersion model. The theories describing the pressure dependence of the velocities (Toksöz et al., 1979; Diallo et al., 2003) are also suitable for deriving the relation between the quality factor and pressure. As the pressure increases, the value of the quality factor increases similarly to the velocity. However, the difficulty is that the determination of attenuation is significantly more difficult than the measurement of velocity. For the laboratory determination of the quality factor (Q) of rocks, Toksöz (1979) developed the method of spectral ratios, a modified version of which was used to evaluate our acoustic P wave measurements. In order to eliminate the effect of geometrical spreading, we also perform a reference measurement on an aluminum sample with the same geometry as the rock sample, since the quality factor of aluminum is very high, and we can use this property well in our calculations. The amplitude spectra of the acoustic waves that can be measured on the samples can be written with the following relations:

$$A_{alu}(f) = G_{alu}(x)e^{-\alpha_{alu}(f)x}e^{j(2\pi ft - k_{alu}x)} \tag{2}$$

$$A_{rock}(f) = G_{rock}(x)e^{-\alpha_{rock}(f)x}e^{j(2\pi ft - k_{rock}x)} \tag{3}$$

where $A_{alu}(f)$ – the amplitude spectrum of the aluminum sample,
$A_{rock}(f)$ – the amplitude spectrum of the sandstone sample,
$G_{alu}(x)$ – the geometric factor of the aluminum sample,
$G_{rock}(x)$ – the geometric factor of the sandstone sample,
x – the length of the samples,
$\alpha_{alu}(f)$ – the frequency-dependent attenuation factor of the aluminum sample,
$\alpha_{rock}(f)$ – the frequency-dependent attenuation factor of the sandstone sample,
k_{alu} – the wavenumber of the aluminum sample,
k_{rock} – the wavenumber of the sandstone sample.

McDonal et al. (1958), Jackson and Anderson (1970) previously showed that in the frequency range 0.1–1 MHz the attenuation factor $\boldsymbol{\alpha}$ is a linear function of frequency, which can be expressed as follows:

$$\alpha(f) = \gamma f\ , \tag{4}$$

where γ – the proportionality factor.

If the geometry of the aluminum sample and the rock sample are the same, the spectral ratio can be written

$$\frac{A_{alu}(f)}{A_{rock}(f)} = e^{-(\gamma_{alu}-\gamma_{rock})fx} \tag{5}$$

because the geometrical spreading on the two samples are nearly the same. Compared to rocks, aluminum is an almost attenuation-free medium ($\gamma_{alu} \approx 0$), therefore:

$$\frac{A_{alu}(f)}{A_{rock}(f)} = e^{\gamma_{rock} f x} \tag{6}$$

Thus, by taking the natural logarithm of this, we can obtain the proportionality factor γ_{rock} of the rock:

$$\gamma_{rock} = \frac{ln\left(\frac{A_{alu}(f)}{A_{rock}(f)}\right)}{x\, f}. \tag{7}$$

Knowing the γ_{rock} quantity, the quality factor can be determined (Toksöz et al., 1979):

$$Q = \frac{\pi}{v\, \gamma_{rock}} \tag{8}$$

where v – the velocity of the acoustic P-wave.

Neglecting phase shift and measurement errors, the logarithm of the spectral ratio calculated as a function of frequency is scattered around the following equalization line:

$$ln\left(\frac{A_{alu}(f)}{A_{rock}(f)}\right)_{str} = \beta f + \delta \tag{9}$$

where β – the inclination angle of the equalization line,
δ – the vertical axis section of the equalization line.

Based on relations (7) and (8), the value of the quality factor can be determined:

$$Q = \frac{\pi x f}{v\, ln\left(\frac{A_{alu}(f)}{A_{rock}(f)}\right)_{str}} \tag{10}$$

4. The results of the measurement evaluation

The data of the velocity of the P wave and the quality factor determined in the pressure function can be seen in *Table 1*.

The data shown in *Table 1* were inverted (the parameters of the model were determined by using a linearized inversion method) according to the single relaxation model. The single relaxation models are described by the following equations:

$$V(\sigma) = V_0 + \Delta V\left(1 - e^{-\lambda\sigma}\right), \tag{11}$$

$$Q(\sigma) = Q_0 + \Delta Q\left(1 - e^{-\lambda\sigma}\right), \tag{12}$$

where V_0 – the velocity at atmospheric pressure,
Q_0 – the quality factor at atmospheric pressure,
ΔV – the difference between the theoretical maximum velocity and the velocity at atmospheric pressure,
ΔQ – the difference between the theoretical maximum of the quality factor and the quality factor at atmospheric pressure,
σ – the value of pressure,
λ – the relaxation factor.

The results of the velocity and quality factor inversion are shown in *Table 2*.

Table 1. *The data of the velocity of the P wave and the quality factor determined in the pressure function*

P [MPa]	V [km/sec]	Q [–]		P [MPa]	V [km/sec]	Q [–]
0.260	4.477	18.896		40.556	4.709	37.451
1.040	4.494	23.889		42.636	4.713	37.363
3.120	4.556	29.940		44.716	4.717	37.487
5.200	4.575	31.703		46.796	4.719	37.496
7.279	4.590	33.136		48.876	4.722	37.408
9.359	4.606	33.767		50.955	4.726	37.629
11.439	4.620	34.709		53.035	4.728	37.396
13.519	4.632	35.130		55.115	4.730	37.756
15.599	4.640	35.530		57.195	4.735	37.708
17.678	4.649	35.993		59.275	4.740	37.758
19.758	4.657	36.132		61.354	4.746	37.576
21.838	4.668	36.354		63.434	4.749	37.645
23.918	4.675	36.452		65.514	4.751	37.621
25.998	4.683	36.563		67.594	4.754	37.777
28.077	4.689	36.930		69.674	4.758	37.696
30.157	4.693	37.112		71.754	4.761	37.713
32.237	4.695	37.233		73.833	4.765	37.747
34.317	4.699	37.241		75.913	4.768	37.765
36.397	4.702	37.423		80.073	4.772	37.725
38.477	4.706	37.499		82.153	4.773	37.721

Table 2. *The results of V and Q inversion using single relaxation*

	Results of V inversion with single relaxation	**Results of Q inversion with single relaxation**
V_0 [km/sec]	4.7638	no data
ΔV [km/sec]	0.2576	no data
Q_0 [–]	no data	19.7833
ΔQ [–]	no data	17.5474
λ [–]	0.0436	0.1972
Dstart [%]	5.3295	44.0272
Dend [%]	0.2448	2.3295
100*Dend/Dstart [%]	4.593	5.291

The *Table 2* shows the values of the (percentage) data distances of the start models and the estimated models. The parameters of the data distances show the efficiency of the inversions. ***Figure 1*** shows the result of the velocity ***(V)*** inversion, and *Figure 2* shows the result of the ***Q*** (quality factor) inversion. Based on ***Table 2*** and the figures (*Figures 1* and *2*), it can be concluded that the inversion of the velocity data was somewhat more effective than the inversion of the quality factor, since the data distance of the velocity result is smaller (*4.593%* of the data distance at the start model) than the quality factor data distance of the result model (*5.291%* of the data distance at the start model).

Since it was visible in the figures of both inversions (*Figures 1* and *2*) that the inversion according to single relaxation describes the pressure dependence inaccurately, the velocity and quality factor data were inverted according to the following double relaxation models:

$$V(\sigma) = A - B_1 e^{-\lambda_1 \sigma} - B_2 e^{-\lambda_2 \sigma}, \tag{13}$$

$$Q(\sigma) = C - D_1 e^{-\lambda_1 \sigma} - D_2 e^{-\lambda_2 \sigma}, \tag{14}$$

where A – the theoretical maximum velocity at very high pressure,
C – the theoretical maximum quality factor at very high pressure,
B_1 – the coefficient of first velocity relaxation,
B_2 – the coefficient of second velocity relaxation,
D_1 – the coefficient of first quality factor relaxation,
D_2 – the coefficient of second quality factor relaxation,
σ – the value of pressure,
λ_1 – the relaxation factor of the first relaxation,
λ_2 – the relaxation factor of the second relaxation.

The results of the double relaxation inversion can be seen in *Table 3*, while the results of velocity inversion is shown in *Figure 3*, and the results of the quality factor inversion is shown in *Figure 4*. Based on *Table 3* and the figures (*Figures 3* and *4*), it can be concluded that the inversion based on double relaxation approximates both the velocity and quality factor data much better than the inversion based on single relaxation.

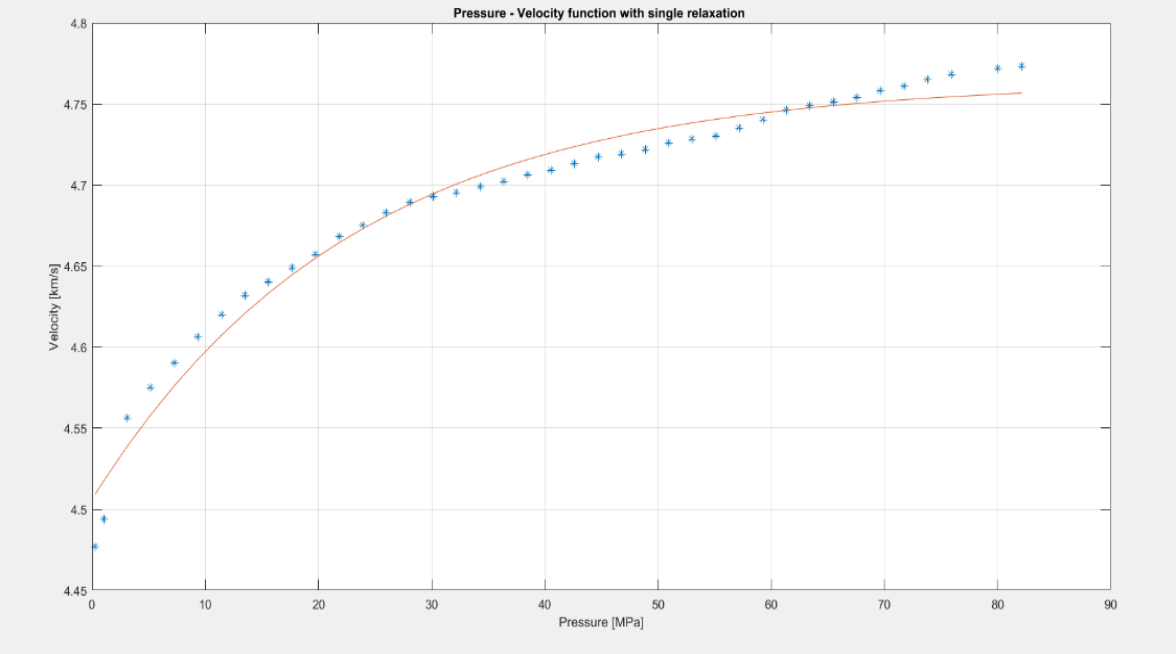

Figure 1. *The result of the velocity inversion using single relaxation*

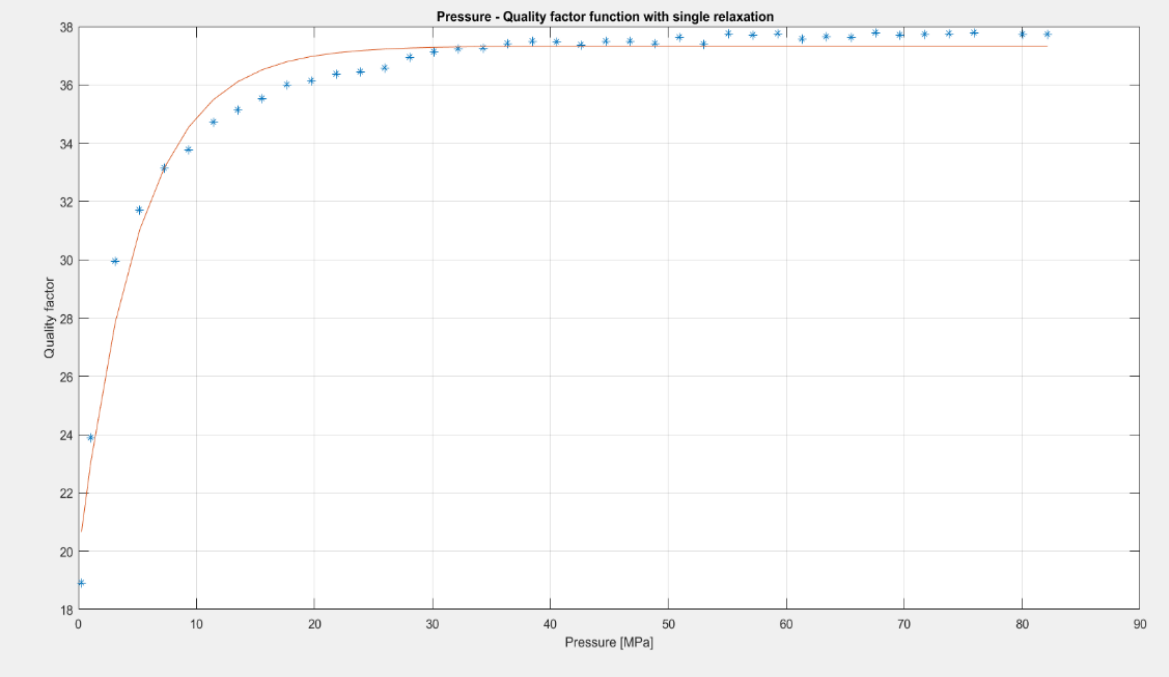

Figure 2. *The result of the quality factor inversion using single relaxation*

Table 3. *The results of V and Q inversion using double relaxations*

	Results of V inversion with double relaxations	**Results of Q inversion with double relaxations**
A [km$_c$/sec]	4.8651	no data
B1 [km$_c$/sec]	0.1333	no data
B2 [km$_c$/sec]	0.2594	no data
C [–]	no data	37.7027
D1 [–]	no data	12.5903
D2 [–]	no data	8.553
λ_1 [–]	0.1856	0.7171
λ_2 [–]	0.0126	0.0863
Dstart [%]	3.5542	7.9644
Dend [%]	0.0864	0.2912
100*Dend/Dstart [%]	2.431	3.656

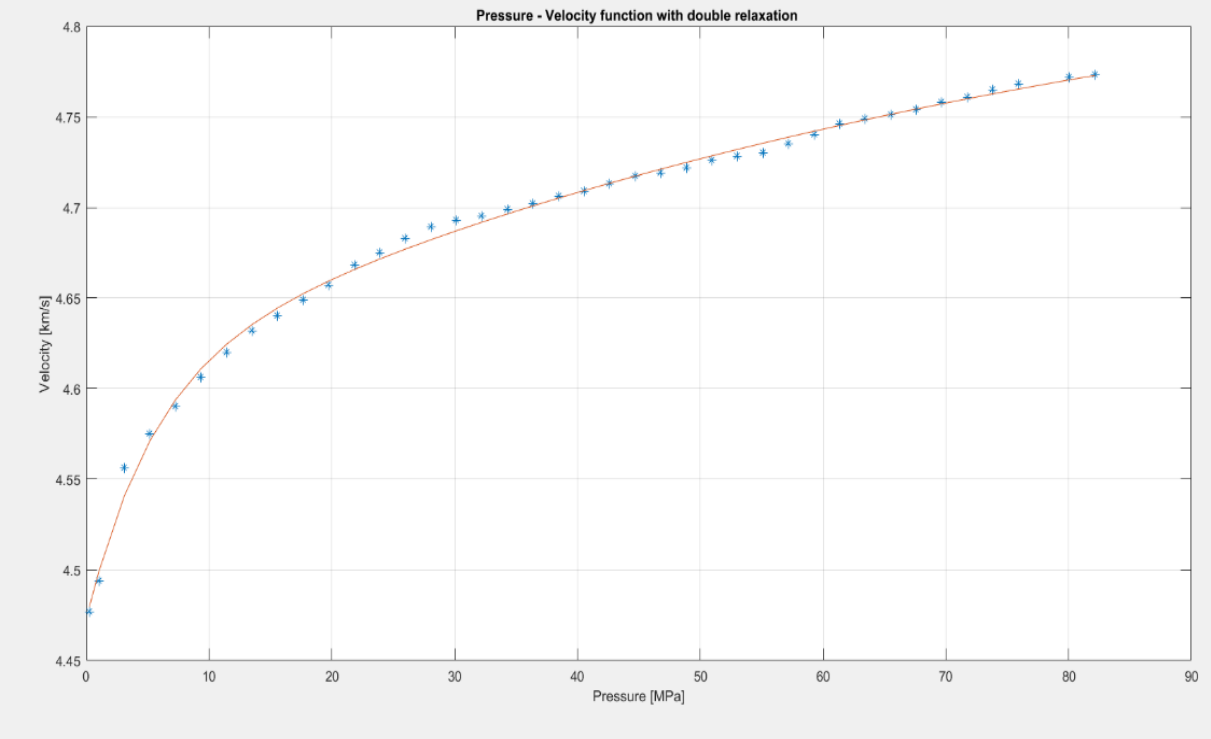

Figure 3. *The result of the velocity inversion using double relaxations*

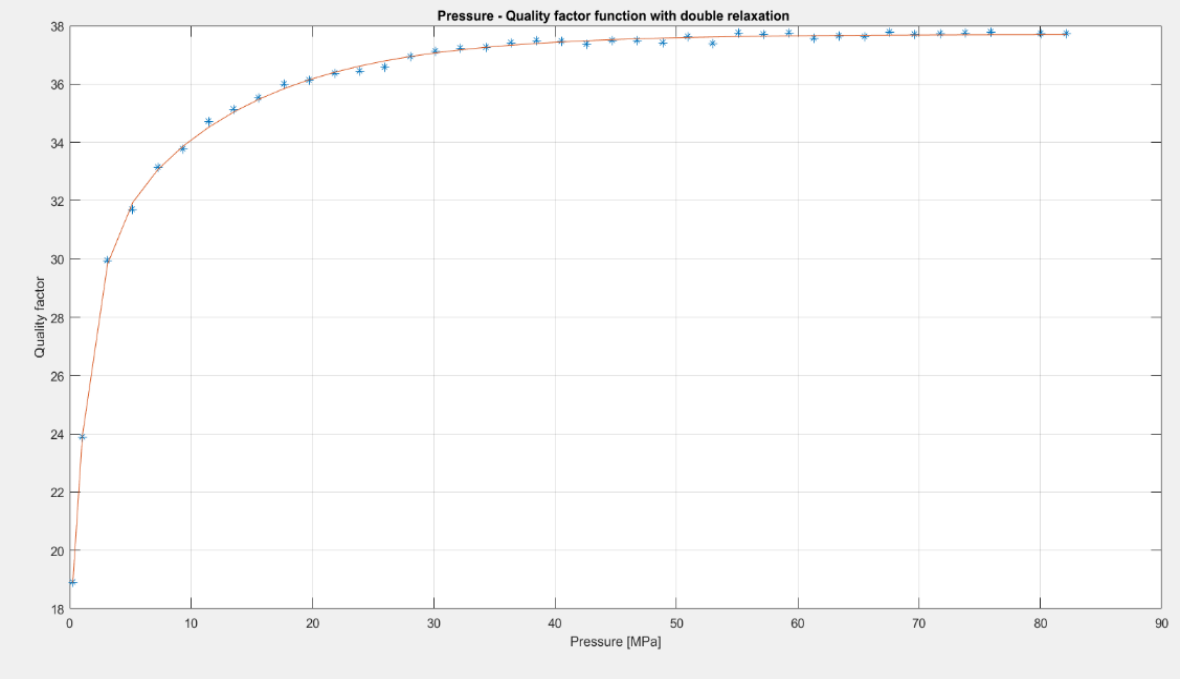

Figure 4. *The result of the quality factor inversion using double relaxations*

The distance between the measured and estimated (by inversion) velocity data obtained with double relaxation is *0.0864%*, which is *2.83* times smaller than the data distance *(0.2448%)* of the inversion according to single relaxation. The data distance *(0.2912%)* of the inversion of quality factor data according to double relaxation is also much smaller (*8* times smaller) than that *(2.3295%)* obtained with single relaxation. Regarding the data distances, the inversion according to double relaxation also gave a better fit (with smaller data distances) in the case of the velocity model than in the case of the quality factor model.

5. Conclusion

The evaluation of the performed acoustic laboratory measurements showed that both the pressure dependence of the P wave velocity data and the pressure dependence of the quality factor data calculated using the modified spectral ratio method show a similar nature. In the range of low pressures, both data (the velocity and the quality factor) increase greatly. As the pressure increases, the rate of increase of both characteristics gradually decreases and thus reaches a maximum value. All this shows that the pressure dependence follows the relaxation model. The results of the inversion according to the relaxation models prove that, in the case of the examined sandstone sample, the double relaxation model gives a much better fit than the single relaxation, which suggests that the pressure dependence is two-component. In the future, our goal is to process the results just presented *(Table 1)* with joint inversion, both for single and double relaxation. Our aim is also to examine the method of calculating the quality factor according to spectral ratio by replacing the measurements on the aluminum sample with the measurements on the rock sample at a given pressure, which can significantly reduce the time of the laboratory measurements.

References

[1] Dócs, R., Baracza, M. K. (2022). A new method of pressure drop modelling in sandstone rocks. *Multidisciplinary Studies*, 12 (3), pp. 264–273. **https://doi.org/10.35925/j.multi.2022.3.24**

[2] Nagy, Zs., Baracza, M. K., Szabó, N. P. (2019). Integrated Pore Pressure Prediction with 3D Basin Modeling. *Second EAGE Workshop on Pore Pressure Prediction*, 19–21 May 2019, Amsterdam, Netherlands, pp. 1–5. **https://doi.org/10.3997/2214-4609.201900513**

[3] Nagy, Zs., Baracza, M. K., Szabó, N. P. (2019). Pore Pressure Prediction In Pannonian Hydrocarbon Reservoir Systems Using An Integrated Interpretation Approach. *Geosciences and Engineering*, 7 (12), pp. 105–115.

[4] Birch, F. (1960). The velocity of compression waves in rocks to 10 kilobars. Part 1. *J. Geophys. Res.*, 65, pp. 1083–1102. **https://doi.org/10.1029/JZ065i004p01083**

[5] Walsh, J. B. and Brace, W. F. (1964). A fracture criterion for brittle anisotropic rock. *J. Geophys. Res.*, 69, pp. 3449–3456. **https://doi.org/10.1029/JZ069i016p03449**

[6] Wyllie, M. R. J., Gregory, A. R., Gardner, G. H. F. (1958). An experimental investigation of factors affecting elastic wave velocities in porous media. *Geophysics*, 23, pp. 459–493. **https://doi.org/10.1190/1.1438493**

[7] Nur, A., Simmons, G. (1969). The effect of saturation on velocity in low porosity rocks. *Earth Planet Sci. Lett.*, 7, pp. 183–193. **https://doi.org/10.1016/0012-821X(69)90035-1**

[8] Stacey, T. R. (1976). Seismic assessment of rock masses. *Proceedings of the Symposium on Exploration for Rock Engineering*, pp. 113–117.

[9] Yu, G., Vozoff, K. and Durney, D. W. (1993). The influence of confining pressure and water saturation on dynamic elastic properties of some Permian coals. *Geophysics*, 58, pp. 30–38. **https://doi.org/10.1190/1.1443349**

[10] Jones, L. A., Wang, H. F. (1981). Ultrasonic velocities in cretaceous shales from the williston basin. *Geophysics*, 46, pp. 288–297. **https://doi.org/10.1190/1.1441199**

[11] Sengun, N. R., Demirdag, A. S. and Yavuz, H. (2011). P-wave velocity and Schmidt rebound hardness value of rocks under uniaxial compressional loading. *Int. J. Rock Mech. Min. Sci.*, 48, pp. 693–696. **https://doi.org/10.1016/j.ijrmms.2011.02.007**

[12] Dobróka, M., Somogyi Molnár, J. (2012). New petrophysical model describing the pressure dependence of seismic velocity. *Acta Geophys.*, 60, pp. 371–383. **https://doi.org/10.2478/s11600-011-0079-0**

[13] Somogyi Molnár, J., Kiss, A., Dobróka, M. (2015). Petrophysical models to describe the pressure dependence of acoustic wave propagation characteristics. *Acta Geod. Geophys.*, 50, pp. 339–352. **https://doi.org/10.1007/s40328-014-0074-4**

[14] Kiss, A. (2018). *Petrophysical investigation of acoustic relaxation phenomena* (in Hungarian). Doctoral dissertation, University of Miskolc, Hungary.

[15] Somogyi Molnár, J., Dobróka, T. E., Ormos, T., Dobróka, M. (2019). Global inversion of pressure dependent acoustic velocity data based on a new double relaxation model. *xProceedings of the 25th European Meeting of Environmental and Engineering Geophysics*, Paper 98906. **https://doi.org/10.3997/2214-4609.201902427**

[16] Dobróka, M., Szabó, N. P., Dobróka, T. E., Baracza, M. K. (2022). Multi-exponential model to describe pressure-dependent P- and S-wave velocities and its use to estimate the crack aspect ratio. *Journal of Rock Mechanics and Geotechnical Engineering*, 14, pp. 385–395. **https://doi.org/10.1016/j.jrmge.2021.08.015**

[17] Knopoff, L. (1965). Attenuation of elastic waves in the earth. In: Mason W. S. (ed.). *Physical acoustics.* Vol 3, Part B. New York: Academic Press, pp. 287–324. **https://doi.org/10.1016/B978-0-12-395669-9.50014-X**

[18] Diallo, M. S., Prasad, M., and Appel, E. (2003). Comparison between experimental results and theoretical predictions for P-wave velocity and attenuation at ultrasonic frequency. *Wave Motion*, 37, pp. 1–16. **https://doi.org/10.1016/S0165-2125(02)00018-5**

[19] Toksöz, M. N., Johnston, D. H. and Timur, A. (1979). Attenuation of seismic waves in dry and saturated rocks: I. Laboratory measurements. *Geophysics*, 44 (4), pp. 681–690. **https://doi.org/10.1190/1.1440969**

[20] Turai-Vurom, B. and Dobróka, M. (2022). Analysis of the full wave spectra of laboratory acoustic measurements. *Multidiszciplináris Tudományok*, 12 (3), pp. 163–173. **https://doi.org/10.35925/j.multi.2022.3.15**

[21] Biot, M. A. (1956). Theory of propagation of elastic waves in a fluid-saturated porous solids, I: Low frequency range. *Journal of the Acoustical Society of America*, 28, pp. 179–191. **https://doi.org/10.1121/1.1908241**

[22] Bland, D. R. (1960). *The theory of linear viscoelasticity*. Oxford: Pergamon Press.

[23] McDonal, F. J., Angona, F. A., Mills, R. L., Sengbush, R. L., Van Nostrand, R. G., and White, J. E. (1958). Attenuation of shear and compressional waves in Pierre shale. *Geophysics*, 23, pp. 421–439. **https://doi.org/10.1190/1.1438489**

[24] Jackson, D. D. and Anderson, D. L. (1970). Physical mechanisms of seismic wave attenuation. *Rev. Geophys. Space Phys.*, 8, pp. 1–63. **https://doi.org/10.1029/RG008i001p00001**